Advances in Water Resources 33 (2010) 1188–1198

Contents lists available at ScienceDirect

Advances in Water Resources

journal homepage: www.elsevier.com/ locate/advwatres

Stochastic analysis of a field-scale unsaturated transport experiment

G. Severino [a,*], A. Comegna [b], A. Coppola [b], A. Sommella [a], A. Santini [a]

[a] Division of Water Resources Management, University of Naples Federico II, Italy
[b] Hydraulics Division, University of Basilicata, Potenza, Italy

ARTICLE INFO

Article history:
Received 13 October 2009
Received in revised form 30 July 2010
Accepted 10 September 2010
Available online 20 September 2010

Keywords:
Solute transport
Field-scale experiment
Stochastic models

ABSTRACT

Modelling of field-scale transport of chemicals is of deep interest to public as well as private sectors, and it represents an area of active theoretical research in many environmentally-based disciplines. However, the experimental data needed to validate field-scale transport models are very limited due to the numerous logistic difficulties that one faces out.

In the present paper, the migration of a tracer (Cl^-) was monitored during its movement in the unsaturated zone beneath the surface of 8 m × 50 m sandy soil. Under flux-controlled, steady-state water flow ($J_w = 10$ mm/day) was achieved by bidaily sprinkler irrigation. A pulse of 105 g/m^2 KCl was applied uniformly to the surface, and subsequently leached downward by the same (chloride-free) flux J_w over the successive two months. Chloride concentration monitoring was carried out in seven measurement campaigns (each one corresponding to a given time) along seven (parallel) transects. The mass recovery was near 100%, therefore underlining the very good-quality of the concentration data-set.

The chloride concentrations are used to test two field-scale models of unsaturated transport: (i) the *Advection-Dispersion Equation* (ADE), which models transport far from the zone of solute entry, and (ii) the *Stochastic-Convective Log-normal* (CLT) transfer function model, which instead accounts for transport near the release zone. Both the models provided an excellent representation of the solute spreading at $z > 0.45$ m (being $z = 0.45$ m the calibration depth). As a consequence, by the depth $z \approx 50$ cm one can regard transport as Fickian. The ADE model dramatically underestimates solute spreading at shallow depths. This is due to the boundary effects which are not captured by the ADE. The CLT model appears to be a more robust tool to mimic transport at every depth.

1. Introduction

In the last decades many issues related to soil and groundwater protection have stimulated theoretical (detailed reviews can be found in [13,43]) as well as experimental (e.g. [6,8,17,20,23,24,28,33,52]) studies on transport phenomena taking place in natural environments. Major progresses have been achieved through parallel studies aiming from one side to set-up experimental techniques for monitoring migration in soils of inorganic, organic dissolved solutes as well as suspended particles (e.g. [7,27]), and to develop from the other proper modelling tools (see, e.g. [12,26]).

The main difficulty relies on the impossibility to describe into a detailed manner the complex (and quite irregular) soil structure. Such a complexity has a direct impact on the reliability of predicting the fate of moving solutes. The tortuosity and considerable irregularity of the flow paths as well as the presence of channels (bio-pores, dead pores, cracks, etc.) slow down (or speed up) advection, and dispersion of migrating solutes (see, e.g. [3]). Even if the governing transport equations have been established (e.g. [2]), solution of them is still a formidable task. One major factor that contributes to the complexity of the problem at stake is the large degree of spatial variability exhibited by natural soils (e.g. see [38,41,51]).

It is a common tenet that heterogeneity has a major influence on transport, and it is responsible of an enhanced (macro)dispersion that cannot be captured by the out-coming of laboratory experiments [12]. Heterogeneity in soils is observed on various scales, ranging from centimeters to tens, and hundreds of kilometers (e.g. [11]). Approaches to model heterogeneity will depend on the scale over which flow, and transport are observed. The basic idea is to construct models which predict the most relevant features (typically moments) of transport.

In the present paper we investigate on the applicability of two of such stochastic models. The main novelty of our contribution (as compared with previous studies on the same topic) relies on the fact that we use a very comprehensive set of real data, along the lines recently traced by Dagan [15] and Neuman [31]. Models selected for testing are calibrated at the depth $z = 45$ cm, and validated at depths different from the calibrating one. The success or failure of a model to describe the data-set will be assessed by means of proper performance indicators. The overall task of this cause/effect approach is to

* Corresponding author. Department of Mechanical and Aerospace Engineering (MAE), University of California, San Diego, USA.
E-mail address: severino@unina.it (G. Severino).

0309-1708/$ – see front matter © 2010 Elsevier Ltd. All rights reserved.
doi:10.1016/j.advwatres.2010.09.004

improve the understanding of solute transport mechanism at the field-scale as influenced by soil properties that are easy to observe/infer from *in situ* measurements.

2. Theoretical background

One of the distinctive features of a soil is the spatial heterogeneity of its hydraulic properties (e.g. [34,35,38,41,49,51]). This spatial heterogeneity is generally irregular (Fig. 1), and it occurs over scales beyond the scope of laboratory samples (e.g. [11]). These features have distinct effects on the spatial distribution of solutes, as it has been observed both in field-scale experiments (e.g. [5,17,36,44]), and by numerical simulations (a wide review can be found in [22,37]).

When we attempt to apply laboratory-scale theories at field (or even larger) scales, we face with a *missing* heterogeneity-issue. In other words, theories/models suitable for laboratory scales (small samples) are generally not applicable at larger scales. To deal with this issue two basic approaches, which we shall briefly recall in the sequel for completeness, have been developed: the physical (i.e. Stochastic), and the system (i.e. Transfer Function) approach.

2.1. Stochastic formulation of solute transport (physical approach)

The formation heterogeneity is set in a mathematical framework by regarding the soil hydraulic properties (such as the hydraulic conductivity, and the water retention function) as *Random Space Functions* (RSFs). As a consequence, the transport equations are of a stochastic nature, and the concentration C is also a RSF. Thus, the aim of the stochastic approach is to evaluate the statistical moments of C given the statistical moments of the hydraulic properties. This is a formidable task, and more often its scope is usually restricted (due to the scarcity of available data) to the computation of the first two moments.

Transport through heterogeneous porous formations can be described as a dispersion-mechanism by continuous motions [12] by following Taylor [47]. For a propagating solute body, the displacement covariance tensor $\mathbf{X}$ of the solute particles can be calculated from the statistics of the velocity field by using the Lagrangian formulation. The solute body is regarded as being composed of many (indivisible) particles, and we assume that a given particle is initially at $\mathbf{a}$, i.e. $\mathbf{X} = \mathbf{a}$ for $t = 0$. Due to the extremely irregular variations of the hydraulic conductivity (see Fig. 1) the concentration "point values" are subjected to considerable uncertainty. As a consequence, we focus our attention on global measures of solute transport, such as the first two-spatial moments of C. These latter represent the information that one can generally achieve from field experiments. For a finite body of a passive solute, with initial constant concentration $C(\mathbf{x}, 0) = C_0$ within a volume V_0, the spatial moments of the distribution of C are given by (see, e.g. [39]):

$$M = \theta C_0 V_0, \qquad \mathbf{R}(t) = \frac{1}{V_0}\int_{V_0} d\mathbf{a}\mathbf{X}(t;\mathbf{a}) \tag{1}$$

$$S_{i,j}(t) = \frac{1}{V_0}\int_{V_0} d\mathbf{a}[X_i(t;\mathbf{a}) - R_i(t)]\left[X_j(t;\mathbf{a}) - R_j(t)\right] (i,j = x,y,z), \tag{2}$$

where M is the total solute mass, $\mathbf{R}$ is the coordinate of the center of gravity of the propagating solute body, whereas $S_{i,j}$ represent the second-order spatial moments (θ being the water content). Under ergodic conditions, which are assumed to prevail if the lateral extent of the solute input zone is sufficiently large compared with the scale of the heterogeneity in the transverse directions [39], one has

$$\mathbf{R}(t) \approx \langle \mathbf{R}(t) \rangle = \mathbf{a} + \mathbf{U}t, \qquad S_{i,j}(t) \approx \langle S_{i,j}(t) \rangle = S_{i,j}(0) + X_{i,j}(t), \tag{3}$$

being $\mathbf{U}$, defined as the ratio between the flux and the mean water content, the water velocity (the operator $\langle\rangle$ stands for the ensemble average), whereas $S_{i,j}(0)$ characterizes the initial dispersion of the plume. The components $X_{i,j}$ of the displacement covariance tensor $\mathbf{X}$ are calculated as $X_{i,j}(t;\mathbf{a}) = \langle X_i'(t;\mathbf{a}) X_j'(t;\mathbf{a}) \rangle$. Hence, under these conditions, the one particle trajectory tensor suffices to characterize (at least up to the second order) spatial moments of a propagating solute body.

Let $f(\mathbf{X};t,\mathbf{a})$ be the *probability density function* (pdf) of $\mathbf{X}$, i.e. $fd\mathbf{X}$ represents the probability of a particle to be within the elementary volume $d\mathbf{X}$ at the time t. The ensemble average $\langle C(\mathbf{x},t) \rangle$ is computed as [12]

$$\langle C(\mathbf{x},t) \rangle = C_0 \int_{V_0} d\mathbf{a} f(\mathbf{x};t,\mathbf{a}). \tag{4}$$

This fundamental result reads as follows: the concentration expected value is obtained via the pdf of the particle trajectory,

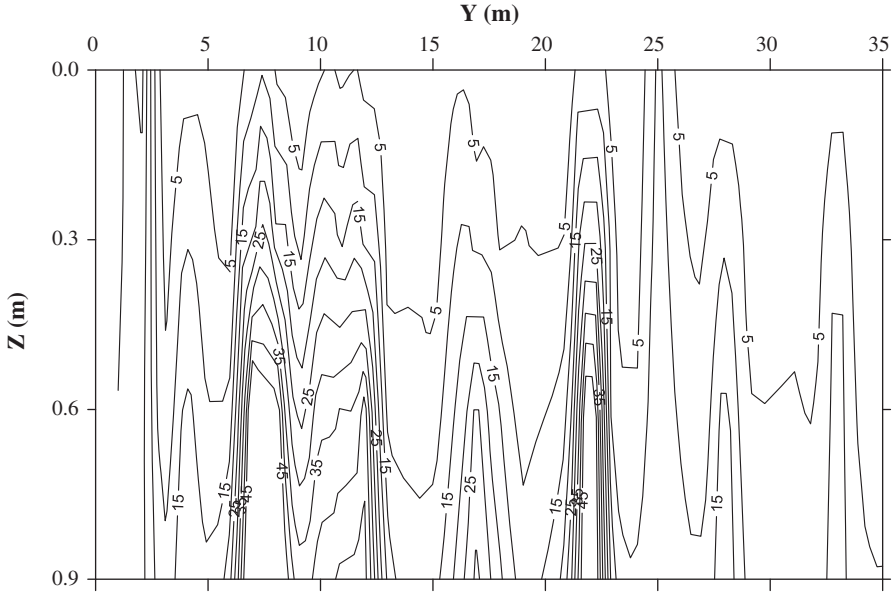

Fig. 1. Distribution of K_s (in cm/h) in a vertical 40 m × 1 m cross section. The values are obtained from 2 × 40 samples taken along 40 profiles at horizontal interval of $\Delta = 1.25$ m, at $z = 30, 90$ cm.

which is regarded as a function of x and t. It is easy to verify that for Gaussian f, the mean $\langle C\rangle$ satisfies the *Advection-Dispersion Equation* (ADE)

$$\frac{\partial}{\partial t}\langle C(z,t)\rangle + U\frac{\partial}{\partial z}\langle C(z,t)\rangle = D\frac{\partial^2}{\partial z^2}\langle C(z,t)\rangle, \tag{5}$$

with

$$U = \frac{d}{dt}\langle X_z(t)\rangle\, D = \frac{1}{2}\frac{d}{dt}X_{zz}(t). \tag{6}$$

Notice that we have limited to consider one-dimensional ADE, since it will be of main concern in the sequel. The main (and usually quite difficult) task is to relate X_{zz} to the Lagrangian velocity field. This line of reasoning has been first pursued by Russo [39], and subsequently generalized by Severino et al. [46] by adapting the approach that originally was proposed by Dagan [10] for transport by groundwater flow. It is beyond the scope of the present paper to go through a detailed discussion of the results. We limit to recall the most relevant (in view of the subsequent discussions) issue: when the centroid of the moving plume has travelled a long-enough distance, dispersion coefficients become constant (see, e.g. [42]), and transport is coined as *Fickian*. In other words, at large depths transport can be modelled by the classical ADE provided that the dispersion coefficient is replaced by $D = \frac{1}{2}\lim_{t\to\infty}\frac{d}{dt}X_{z,z}(t)$. Furthermore, it has been demonstrated by Severino et al. [46] that the required travel-distance to attain the Fickian regime is a formation-property, irrespective whether the porous medium is fully or partially saturated.

Finally, it is worth reminding that the governing equation for $\langle C\rangle$ is generally non local (for a wide review, see [32]). One way to circumvent such a non-locality is the above mentioned Lagrangian approach. When such an approach is not warranted, alternative techniques, most of which are described by Dentz and Tartakovsky [16], can be used.

2.2. Transfer function formulation of solute transport (system approach)

This approach relies on the application of the principles of superposition, and mass balance to a finite volume of soil bounded by a top-surface through which solute enters, and an exit one through which it leaves [26]. Transport is preliminarily characterized via an *ad hoc* experiment/measurement in which a narrow pulse of a tracer mass M is added at the inlet of the volume, and it is recovered at the outflow surface as function of the time.

The recorded outflow is sought in a probabilistic sense as follows: if during the time period $\triangle t_j = t_{j+1} - t_j$ a fraction $\frac{m_j}{M}$ of the total input mass M crosses the outflow surface located at a given depth z, then

$$\mathrm{P}\left(t_j<t<t_{j+1}\right) = F\left(t_{j+1}\right) - F\left(t_j\right) \approx \frac{m_j}{M} \tag{7}$$

where $F = F(t)$ is the probability that a solute added at the inlet at $t = 0$ will cross the outflow surface at a time less or equal to t. If the flux J_w is steady, then

$$m_j \approx J_w\, \overline{C}\left(z,t_j\right)\triangle t_j, \tag{8}$$

where $\overline{C}\left(z,t_j\right)$ refers to the average out-flowing concentration (defined as ratio between the solute mass crossing a unit area to the water volume crossing the same area) between t_j and t_{j+1}.

Eqs. (7) and (8) enable one to establish a relationship between the observable concentration $\overline{C}$, and the travel time $f = f(t)$ pdf. Indeed, by recalling that this latter is defined as

$$f(t) = \lim_{\triangle t\to 0}\frac{F(t+\triangle t) - F(t)}{\triangle t} = \frac{d}{dt}F(t), \tag{9}$$

and by combining with Eqs. (7)–(9), we may write

$$f(t) = \frac{\overline{C}(z,t)}{\int_0^\infty dt\,\overline{C}(z,t)}. \tag{10}$$

This fundamental result reads as follows: the normalized outflow concentration of an experiment in which a narrow pulse is added to the inlet of a transport volume (under steady water flow conditions) is equal to the travel time pdf of that volume.

By using the superposition principle (for details see [26]) we may write the concentration for an arbitrary input concentration $\overline{C}(0,t)$ as

$$\overline{C}(z,t) = \int_0^t dt'\, C(0,t-t')f(z,t'). \tag{11}$$

Eq. (11) may be interpreted as follows: the solute flux arriving at the outflow at the time t contains solutes that entered the control volume at all the times less than t. In particular, if a particle enters at the time $t-t'$, it has the probability $f(t')\mathrm{d}t'$ of having a travel time t', or of exiting the control volume at the time t. The integral is just the cumulant of all the possible contributions from travel times t' between 0 and t.

The transfer function framework has some advantages, and some disadvantages over the physical approach. The travel time $f(t)$ records the transfer features of the medium completely, and therefore it is valid for all (linear) transport processes: it does not require any process assumption. To the contrary, it merely predicts concentrations at the outflow, which means that it cannot be used (unless some further hypotheses are invoked) to predict the outflow concentrations at any other depth within/beyond the control volume. Thus, extension of the approach to depths different from that at which the transfer function is calibrated requires an assumption concerning the transport process.

At field-scale the so-called *Stochastic-Convective Transfer Function* revealed successful into recovering the outcome of several field-scale transport experiments (e.g. [6,50]). It is assumed that solutes are confined in isolated stream-tubes. As a consequence, the probability that a solute particle will reach a depth z in a time less or equal to t must be the same probability that it will reach the calibration depth ℓ in a time less than or equal to $\frac{\ell}{z}t$, i.e.

$$\mathrm{P}(z,t) = \mathrm{P}\left(\ell,\frac{\ell}{z}t\right). \tag{12}$$

Now, by accounting for Eqs. (9) and (12), one has

$$f(z,t) = \frac{d}{dt}\mathrm{P}(z,t) = \frac{d}{dt}\mathrm{P}\left(\ell,\frac{\ell}{z}t\right) = \frac{\ell}{z}f\left(\ell,\frac{\ell}{z}t\right). \tag{13}$$

Eq. (13) establishes a relation between the pdf at any depth $z \neq \ell$. To model the travel time (Eq. (13)) at the calibration depth ℓ, Jury [25] used the log-normal distribution

$$f(\ell,t) = \frac{1}{\sqrt{2\pi}\sigma_\ell t}exp\left[-\left(\frac{\ln t-\mu_\ell}{\sqrt{2}\sigma_\ell}\right)^2\right], \tag{14}$$

where $\mu_\ell = \ln\left[\frac{<t>}{\sqrt{1+\mathrm{CV}^2(t)}}\right]$, and σ_ℓ represent the mean and variance of the random variable $ln\ t$, respectively. When the stochastic-convective hypothesis is applied to Eq. (14), the log-normal travel time at any depth z writes as

$$f(z,t) = \frac{1}{\sqrt{2\pi}\sigma_\ell t}\exp\left\{-\left[\frac{\ln(t\ell/z)-\mu_\ell}{\sqrt{2}\sigma_\ell}\right]^2\right\}, \tag{15}$$

which will be referred hereafter as *Convective Log-normal Transfer* (CLT) function. Similarly to the physical approach, here the normalized concentration is completely characterized by the mean μ_ℓ, and the standard deviation σ_ℓ measured at the calibration depth $z=\ell$.

In the sequel, we shall apply the ADE as well as the CLT models to analyze a recently conducted unsaturated field-scale tracer transport.

3. The field-scale transport experiment

The experimental-field, which is located at the Ponticelli-site (nearby Naples, Italy), is a sandy soil. The soil texture in the upper 1.00 m was studied in detail by sampling at 0.20 m increments in several (randomly selected) locations across the field. The results of the textural analysis with the corresponding soil texture classification are listed in Table 1. The main feature is that the soil is macroscopically homogeneous up to 0.80 m, with a layer of finer textured (loamy) soil at $0.80 \div 1.00$ m. The soil resulted structureless in the sand component, and sub-angular blocky in the finer textured component. Measurements of the soil bulk density ρ up to 1.00 m (with 0.30 cm depth intervals) at various locations across the field had mean and standard deviation equal to 1.01 g/cm^3 and 0.13 g/cm^3 (i.e. CV(ρ) = 13%), respectively.

The saturated hydraulic conductivity K_s was measured along 40 profiles in the field by using the auger-hole method [1]. Because in the auger-hall method the sampled volume has the same size of the laboratory-scale samples, such measurements of K_s can be considered homogeneous to those obtained by laboratory techniques (e.g. by means of permeameters). The distribution of measured values was normal with mean 0.13 cm/min, and coefficient of variation equal to 24%. In addition, K_s was measured upon 80 soil samples taken at $z=0.30$ cm, and $z=0.90$ cm (every 1.25 m) along a (50 m long) transect parallel to the field where the transport experiment was carried out. The measured (by means of the constant-head permeameter method) values lead to the following results: mean 0.35 cm/min, and coefficient variation CV(K_s) = 1.15. A preliminary analysis of the spatial structure of K_s revealed a horizontal correlation integral scale approximately equal to 7 m. In Fig. 1 we have depicted contour plots of K_s (cm/h) as measured across a vertical (40 m × 1 m) cross section. The irregular, ostensibly erratic, variations of K_s are clearly evident.

The experimental plot (8 m width × 50 m long), equipped by a sprinkler irrigation system, was set-up under a greenhouse in order to prevent additional (due to rain-events) water supplies. The sprinkler irrigation system supplied a flux of 10 mm/day. The coefficient of uniformity of the sprinkler system was 87%. It was estimated by catch-cans placed in the vertexes of a regular (1 m × 1 m) grid covering the whole plot. Meteorological data were also *in situ* measured by a standard weather-box recording temperature, relatively humidity, and potential evapotranspiration (ET). In particular, the ET-values were used to estimate the net amount of water entering the soil.

3.1. Experimental methodology

The field was regularly irrigated for nine weeks prior to the tracer application to leach the soil of residual salts, and to achieve a reasonably time invariant (at least up to $z=2$ m) water-content profile. The mean water content $\langle\theta\rangle$, measured at depth intervals of 0.15 m (and several times) is depicted in Fig. 2. Higher values of $\langle\theta(z)\rangle$ were detected at higher depths (say for $z>0.55$ m). This is due to the presence (see Table 1) of a different sub-layer. The coefficient of variation CV(θ) was always less than 20% (Table 2). While such a variability of the mean water content has a small impact upon the soil hydraulic properties, it has a tremendous influence on solute transport. This issue will be fully addressed later on when discussing (in Section 4) the out-coming of the transport experiment.

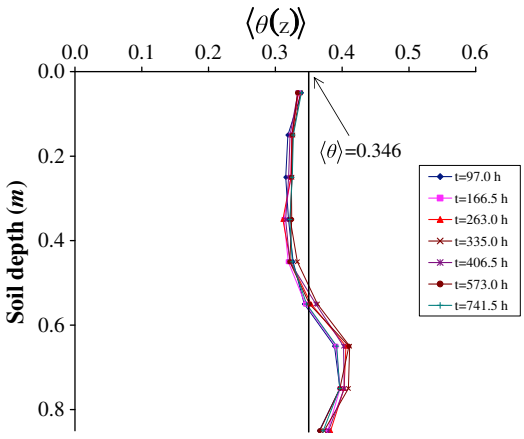

Fig. 2. Average water-content profiles as function of the depth, at the sampling times.

As for the chloride application, 45 g of KCl were dissolved in 1l of deionized water, and subsequently siphoned into the irrigation system followed by an additional 5 mm of water supply. The resulting applied (at the surface) mass was $M_0 = 105$ g/m^2 (corresponding to an input concentration equal to 21 g/l). Given the small interval (of the order of minutes) of the solute application as compared with the advective characteristic time (of the order of days), the boundary condition can be well approximated by a Dirac-pulse, i.e.

$$C(0,t) = \frac{M_0}{U_0}\delta(t) \tag{16}$$

being U_0 the ratio between the water flux, and the mean water content at the soil surface $z=0$. The soil was then leached down to 2.0 m over the next two months by irrigation of 10 mm of applied chloride-free water each day. Monitoring of the chloride concentration was carried out in seven measurement campaigns (corresponding to 97, 167, 263, 335, 407, 573, 742 h) along seven parallel transects (each one 40 m long), at fixed horizontal distance of 1 m (Fig. 3a). For each transect, nine depths ($z=0.10;0.20;0.30;0.40;0.50;0.60;0.70;0.80;0.90$ m) were sampled (Fig. 3b). This was repeated for each transect along 40 vertical profiles (1.25 m away from the other) so that at the end of a single campaign 9 × 40 samples were taken. A considerable effort was made into maintaining the same sampling methodology over the duration of the experiment. Typically, each campaign required 4 h to be completed. The total number of soil samples (taken by an Edelmann-type auger) was 2500.

Table 1
Soil particle size distribution, and statistics (i.e. mean and standard deviation) of the saturated hydraulic conductivity K_s of the experimental plot.

Horizon	Depth (cm)	Coarse sand 2>d≥0.2 mm	Fine sand 0.2>d≥0.002 mm	Silt 0.002>d≥0.0002 mm	Clay d<0.0002 mm	K_s (cm/h)	
						Mean	Stand dev
Ap	0–20	30.0	50.0	12.0	8.0	8.82	3.29
BW	20–50	30.0	53.0	12.0	5.0	7.78	1.66
BC	50–80	34.0	48.0	12.0	6.0	–	–
C	80–100	25.0	63.0	7.0	5.0	–	–

Table 2
Mean $\langle\theta\rangle$, and coefficient of variation CV(θ) of the water content versus the depth at different times.

Time (h)	Mean/ coefficient of variation	Depth (m)							
		15.0	25.0	35.0	45.0	55.0	65.0	75.0	85.0
97.0	$\langle\theta\rangle$	0.32	0.32	0.32	0.33	0.34	0.39	0.40	0.37
	CV(θ)	0.04	0.06	0.07	0.07	0.08	0.10	0.11	0.13
166.5	$\langle\theta\rangle$	0.32	0.32	0.31	0.32	0.35	0.39	0.40	0.38
	CV(θ)	0.05	0.05	0.06	0.07	0.11	0.14	0.18	0.13
263.0	$\langle\theta\rangle$	0.32	0.32	0.31	0.32	0.35	0.41	0.40	0.38
	CV(θ)	0.05	0.10	0.10	0.06	0.07	0.16	0.15	0.14
335.0	$\langle\theta\rangle$	0.33	0.32	0.32	0.33	0.36	0.41	0.41	0.37
	CV(θ)	0.04	0.04	0.06	0.05	0.11	0.16	0.16	0.17
406.5	$\langle\theta\rangle$	0.32	0.32	0.32	0.32	0.36	0.40	0.40	0.38
	CV(θ)	0.04	0.04	0.05	0.11	0.12	0.14	0.13	0.15
573.0	$\langle\theta\rangle$	0.33	0.32	0.32	0.32	0.35	0.41	0.40	0.37
	CV(θ)	0.05	0.05	0.05	0.07	0.09	0.14	0.17	0.19
741.5	$\langle\theta\rangle$	0.33	0.33	0.32	0.33	0.35	0.39	0.40	0.37
	CV(θ)	0.05	0.04	0.05	0.07	0.08	0.14	0.19	0.20

From each soil sample 100 g were immediately taken, and sealed in a plastic bag. Upon such sub-samples we determined: (i) the gravimetric water content; (ii) the soil particles size by the hydrometer method (e.g. [21]); and (iii) the organic carbon [30]. In order to determine the chloride concentration, samples were dried (in an oven at 105 °C), and then sieved by a grid 2 mm × 2 mm. Hence, a mixture consisting of 50 g of dried sample, and 100 ml of deionized water was prepared, shaken, and filtered by using a 0.45 μm cellulose-nitrate membrane filter. In the extracted liquid component, the Cl^- concentration was measured by using an ion-specific electrode setup. The gravimetric concentration C_g was determined as mass of chloride per mass of dried soil. Hence, the concentration C (mass of chloride per volume of soil) was computed as $C = \rho C_g$.

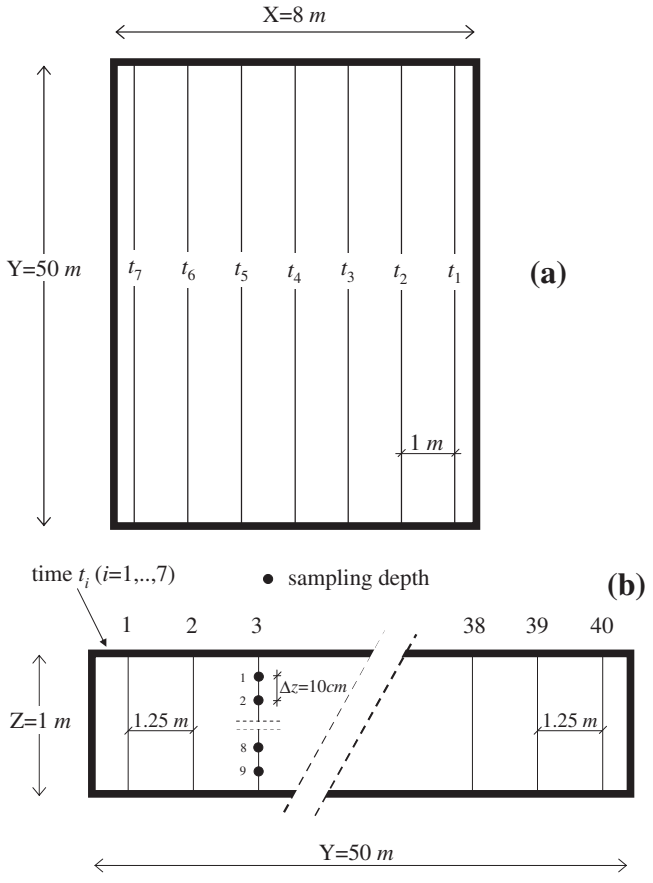

Fig. 3. Sketch of the field plot (at the Ponticelli-site) showing the locations at the several times t_i as well as the sampling depths.

3.2. Mass recovery

The recovered mass may be used to gauge the efficiency of the sampling technique as well as the reliability/quality of the concentration data. The recovered specific (i.e. per unit area) solute mass M_r along the depth was determined as follows

$$M_r = \sum_{i=1}^{N} C(z_i)\theta_i \Delta z, \tag{17}$$

where $C(z_i)$ is the concentration of the ith of $N = 40$ sampling intervals of Δz length, and θ_i the volumetric water content at z_i (Fig. 3b).

In the Table 3 we have reported M_r as percentage of the total initially applied chloride mass $M_0 = 0.105$ kg/m^2. The recovery mass lies between 80.5% and 101.3%. In particular, the mass recovery exceeds at two depths (i.e. $z = 0.15$ m and $z = 0.65$ m) the maximum value of 100%. Such an anomaly is likely due to a residual chloride mass which was not completely removed by the flushing prior to the chloride application. Indeed, as it can be argued by inspection of Fig. 1, at $z \approx 0.70$ m the saturated hydraulic conductivity (and *a fortiori* the hydraulic conductivity) drastically reduces. As a consequence, the chloride-free water that was applied before initiating the experiment was probably not enough to push downward $z = 1$ m the residual chloride. Another additional explanation can be addressed to some (very small) inaccuracy in the numerical evaluation of Eq. (17).

3.3. Concentration data

Here the local concentration value $C = (1/\Omega)\int d\mathbf{x} c(\mathbf{x}, t)$ (being c the point value) is sought as space average over a support Ω centered at $\mathbf{x}$. If Ω is small enough, then C can be considered as "point value." The high variability associated to the solute propagation in the field site may be visualized by examining (Fig. 4) the concentration profiles monitored at the different times. The uncertainty in transport is highlighted by the very large fluctuations of local measurements (discrete symbols) as compared with the mean (continuous line) values. While the uncertainty in the local concentration measurements has been reduced by repeating (5 times) for each sub-sample the chloride detection (and subsequently taking the average), the uncertainty in the field average concentration might be "in principle" assessed only by repeating the same experiment. In fact, while the above recalled stochastic models refer to all possible realizations, the field data are computed as spatial averages. The identification of ensemble average, i.e. $\langle C\rangle$, from the spatial one, i.e. $\overline{C}$, is possible under the ergodicity-hypothesis (for a wide discussion on this issue, see [12]). The pragmatic approach adopted here is to presume that ergodicity holds (at the least up to the second-order moments of the concentration data), and to check it *a posteriori* by comparing the model prediction with real data. Nevertheless, the attainment of the ergodic-issue in the case of the Ponticelli-site has been already assessed for flow by Severino et al. [45]. For these reasons, we shall assume that $\overline{C} \approx \langle C\rangle$.

Table 3
Estimated and recovered mass expressed as a percentage between M_r and M_0.

Depth (m)	Solute mass (kg/m^2)	Recovered M_r/M_0 (%)
0.15	0.106	101.1
0.25	0.103	97.8
0.35	0.097	92.4
0.45	0.102	97.4
0.55	0.103	98.0
0.65	0.106	101.3
0.75	0.098	93.8
0.85	0.085	80.5

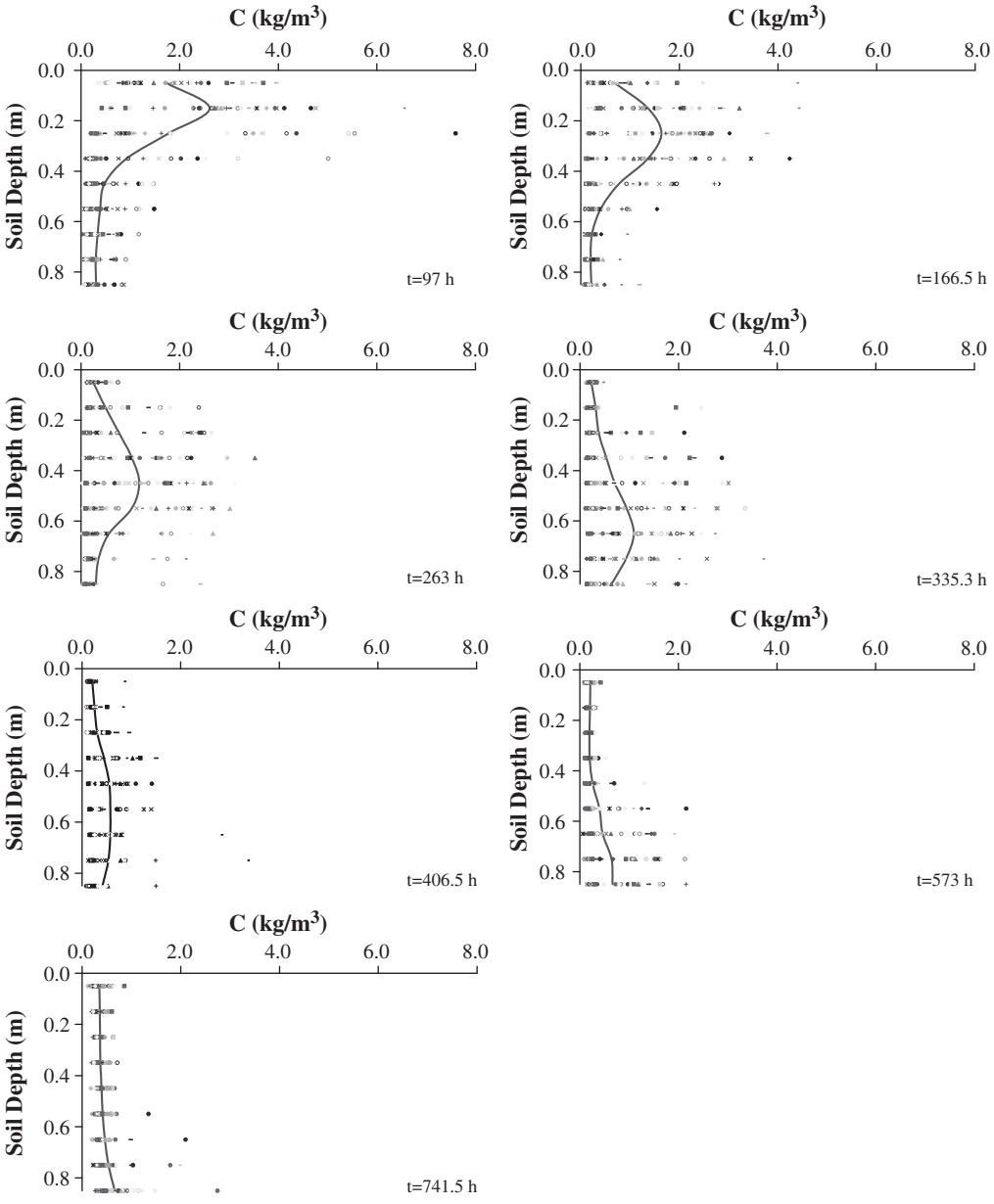

Fig. 4. Measured (discrete points), and mean (continuous line) chloride concentration at the sampling times.

Notice in Fig. 4 that the peak of the mean concentration decreases as time elapses. As a consequence, the concentration profile becomes flatter, and wider. The peaks are captured at all (except at the last) sampling time. In the Fig. 4 it is also seen that fluctuations are larger around the centroid of the concentration profiles in agreement with theoretical studies [9,39,46,52]. The most striking (and quite important for the modelling point of view) issue is that, unlike the water content, the range of the coefficient of variation was between 26% and 170% (Table 4).

An interesting way to look at the pattern of the solute propagation is by means of the "so-called" mobile transport volume

$$\theta_m = J_w \frac{T_1}{z}, \tag{18}$$

where T_1 is the arrival (at the depth z) time of the center of gravity of the concentration profile. Indeed, θ_m can be considered as the applied water flux J_w divided by the average solute velocity. The quantity (Eq. (18)), which in the case of the Ponticelli experiment had a mean equal to 0.232, can be compared with the mean water content $\langle\theta\rangle = 0.346$. In soils, the mean water content $\langle\theta\rangle$ may differ from $\langle\theta_m\rangle$ for a variety of reasons. In our case, since it results $\langle\theta_m\rangle < \langle\theta\rangle$, exclusion anionic processes due to negatively charged mineral are likely to be present. As a consequence, the water volume $z^*\langle\theta_m\rangle$ required to push downward the center of gravity of the concentration profile at a given depth z^* is less than the average one, i.e. $z^*\langle\theta\rangle$. This suggests that a large portion of solutes is moving downward at higher velocities, therefore supporting the use of one-dimensional models. It is worth emphasizing that such a conclusion is sought in a mean sense. Indeed, as it will be clearer later on, the use of one-dimensional models is not authorized in the very shallow depths due to the occurrence of the lateral transport.

4. Discussion

The concentration data of the Ponticelli-site enable one to analyze the impact of the medium heterogeneity upon the solute spreading mechanisms at field-scale. A major question which may be addressed by means of this data-set is the analysis of the structure of the

Table 4
Mean $\langle C\rangle$ and coefficient of variation CV(C) of chloride concentration at different depths, and sampling times.

Time (h)	Mean/ coefficient of variation	Depth (m)							
		0.15	0.25	0.35	0.45	0.55	0.65	0.75	0.85
97.0	$\langle C\rangle$	0.83	0.57	0.31	0.16	0.13	0.13	0.12	0.11
	CV(C)	0.52	1.03	1.36	1.09	0.81	0.76	0.69	0.79
166.5	$\langle C\rangle$	0.44	0.53	0.44	0.26	0.14	0.09	0.08	0.08
	CV(C)	0.77	0.57	0.74	1.10	1.48	0.91	0.69	1.19
263.0	$\langle C\rangle$	0.16	0.24	0.32	0.38	0.36	0.23	0.14	0.11
	CV(C)	1.18	1.16	0.88	0.74	0.91	1.16	1.31	1.70
335.0	$\langle C\rangle$	0.10	0.12	0.17	0.23	0.34	0.45	0.37	0.24
	CV(C)	1.41	1.07	1.27	1.11	0.93	0.68	0.79	0.79
406.5	$\langle C\rangle$	0.08	0.10	0.14	0.17	0.20	0.23	0.21	0.16
	CV(C)	0.84	0.61	0.75	0.67	0.70	0.81	1.04	0.90
573.0	$\langle C\rangle$	0.07	0.06	0.06	0.08	0.14	0.20	0.26	0.25
	CV(C)	0.29	0.26	0.39	0.82	1.06	1.10	0.95	0.84
741.5	$\langle C\rangle$	0.12	0.12	0.12	0.13	0.14	0.18	0.21	0.26
	CV(C)	0.33	0.30	0.33	0.29	0.43	0.66	0.73	0.84

macrodispersion as it evolves from the soil surface. Toward this aim, we shall adopt the two previously revisited models, i.e. (i) the ADE model (Eq. (5)), and (ii) the CLT model (Eq. (15)). To test model predictions, we shall use the mean concentration profiles. In addition, a moment analysis will be conducted to obtain physical insights on the macrodispersion evolution.

The scaled (i.e. divided by the applied mass M_0 over the infiltrating volumetric rate) breakthrough curves at eight control depths (i.e. $z=0.15;0.25;0.35;0.45;0.55;0.65;0.75;0.85$ m) are plotted (discrete symbols) in Fig. 5 together with the CLT (dashed line), and the ADE (continuous line) predicted distributions. To minimize the impact of sampling errors, the mean concentration was computed by averaging $n=40$ local profiles (each one corresponding to a given sampling campaign) as follows:

$$\overline{C}(z,t)=\frac{\sum_{i=1}^{n}\theta_i(z,t)C_i(z,t)}{n\langle\theta(z)\rangle}. \tag{19}$$

It is seen from Eq. (19) that the weight assigned to each concentration measurement is $\frac{\theta_i(z,t)}{n\langle\theta(z)\rangle}$, being $\theta_i(z,t)$ the local water content at given depth z and time t, whereas $\langle\theta(z)\rangle$ represents the mean water-content profile (Fig. 2). Such a choice is motivated by the fact that in this way we can account for the impact of the water-content fluctuations (e.g. [21]).

The parameters of the ADE and CLT models have been determined by the least square optimization algorithm. The optimization procedure lead to the following values: 1) $U=15.8\cdot10^{-4}$ m/h, and $D=9.5\cdot10^{-5}$ m^2/h; 2) $\mu_{\chi}=5.42$ and $\sigma_{\chi}=0.51$. Two different calibration procedures were used with the ADE: either fitting both U and D, or just fitting D, and estimating U as ratio between the flux J_w, and the mean water content $\langle\theta\rangle$. In this second case, even if the optimization was satisfactory (in terms of objective function), it turned out that the agreement of the model with data, that was tested by means of indicators (Eqs. (20)–(22)), was very poor. This is explained by the fact that, even if the advective velocity U can be considered constant in the time, it cannot be treated as uniformly distributed. This addresses *a posteriori* the impact of the increase in the mean water content (see Fig. 2) due to the finer stratification at $z\geq0.80m$. For this reason, U cannot be regarded as a given (i.e. estimated from simultaneous measurements of the flux, and the water content) parameter, but instead it has to be calibrated.

At $z\geq0.55$ m the agreement between the data, and the CLT model is slightly better than the one with the ADE model (Fig. 5b). In particular, the CLT model predicts the early arrivals, and the marked tailing at the deepest depths. Instead, both the models are not in a good agreement with data at $z=0.15$ m (Fig. 5a). More precisely, while the ADE model under-predicts tracer dispersion (and concurrently it over-predicts peak concentration), the CLT one underestimates the early arrivals. The reason is that close to the soil surface transverse (typically radial) transport is not negligible. Indeed, it is well-known that radial flows (unlike mean uniform ones) significantly enhance mixing. As a consequence, peaks are slightly overpredicted at the shallow depths. A similar argument applies to the CLT model. In fact, this latter assumes that transport takes place in isolated vertical columns, and therefore it underestimates the travel times due to the neglect of lateral movements.

The predicting performances of the previous models are quantified here by using three different criteria, namely: i) the maximum error (ME), ii) the root mean square error (RMSE), and iii) the model efficiency (EF) [29],

$$\mathrm{ME}=\max_{i=1,\ldots,n}|\mathrm{P}_i-\mathrm{M}_i| \tag{20}$$

$$\mathrm{RMSE}(\%)=100\sqrt{\frac{\sum_{i=1}^{n}(\mathrm{P}_i-\mathrm{M}_i)^2}{\sum_{i=1}^{n}\mathrm{M}_i}} \tag{21}$$

$$\mathrm{EF}=1-\frac{\sum_{i=1}^{n}(\mathrm{P}_i-\mathrm{M}_i)^2}{\sum_{i=1}^{n}(\overline{\mathrm{M}}-\mathrm{M}_i)^2}, \tag{22}$$

where P_i and M_i represent predicted and measured solute concentrations, respectively, whereas $\overline{\mathrm{M}}=(1/n)\sum_i\mathrm{M}_i$ is the mean of the measured concentration. The ME and the RMSE are the maximum error, and the average deviation between measurements and prediction. Instead, the EF (also known as *Nash–Sutcliffe*) parameter is a measure of the model capability to predict the measured concentrations. For an ideal prediction, the values of Eqs. (20)–(21) should be 0, whereas EF = 1 (when EF attains negative values, a poor fitting is obtained). Inspection of Table 5 shows that both the models perform quite well for $z\geq55$ cm (Fig. 5b). The poor agreement of the theoretical predictions close to the soil surface (Fig. 5a) is also quantitatively confirmed by the values of ME, RMSE, and EF.

The ADE-based prediction at $z=0.15$ m provides the most graphic illustration of the problem in estimating the extent of solute spreading when Fickian transport is mistakenly assumed. Indeed, Fig. 5 shows that the variance of real data is much greater than that the ADE model can account for. As it will be clearer later on, the concentration profiles at $0\leq z\leq0.40$ m offers a visual confirmation that Fickian transport has not yet fully-attained. In fact, if the dispersivity had already approached an asymptotic value by such a depth, then the ADE projection of the solute spreading using the parameters calibrated at $z=0.45$ m should have been very good. Since the predictions at depths larger than 0.45 m are in a good agreement with data (Fig. 5b), we argue that by $z>0.45$ m transport can be regarded as Fickian. It should be noted that the CLT performed almost equally well into predicting transport both at large, and small depths. This is not surprising, since the applicability of the CLT function model is not restricted to the asymptotic regime. However, the error analysis (Table 5) showed the overall superiority of ADE with respect to the CLT function model.

An alternative characterization to transport can be achieved by means of moments (e.g. [39,40,42,46]). Generally, moments are random quantities, but they are approximately equal to their mean values; that is, they satisfy the ergodic hypothesis [39]. Thus, by

Fig. 5. Scaled measured (circles) concentration data versus theoretical (lines) predictions as function of the elapsed time (h) at eight different depths. Case a): $z\leq0.45$ m and case b): $z>0.45$ m.

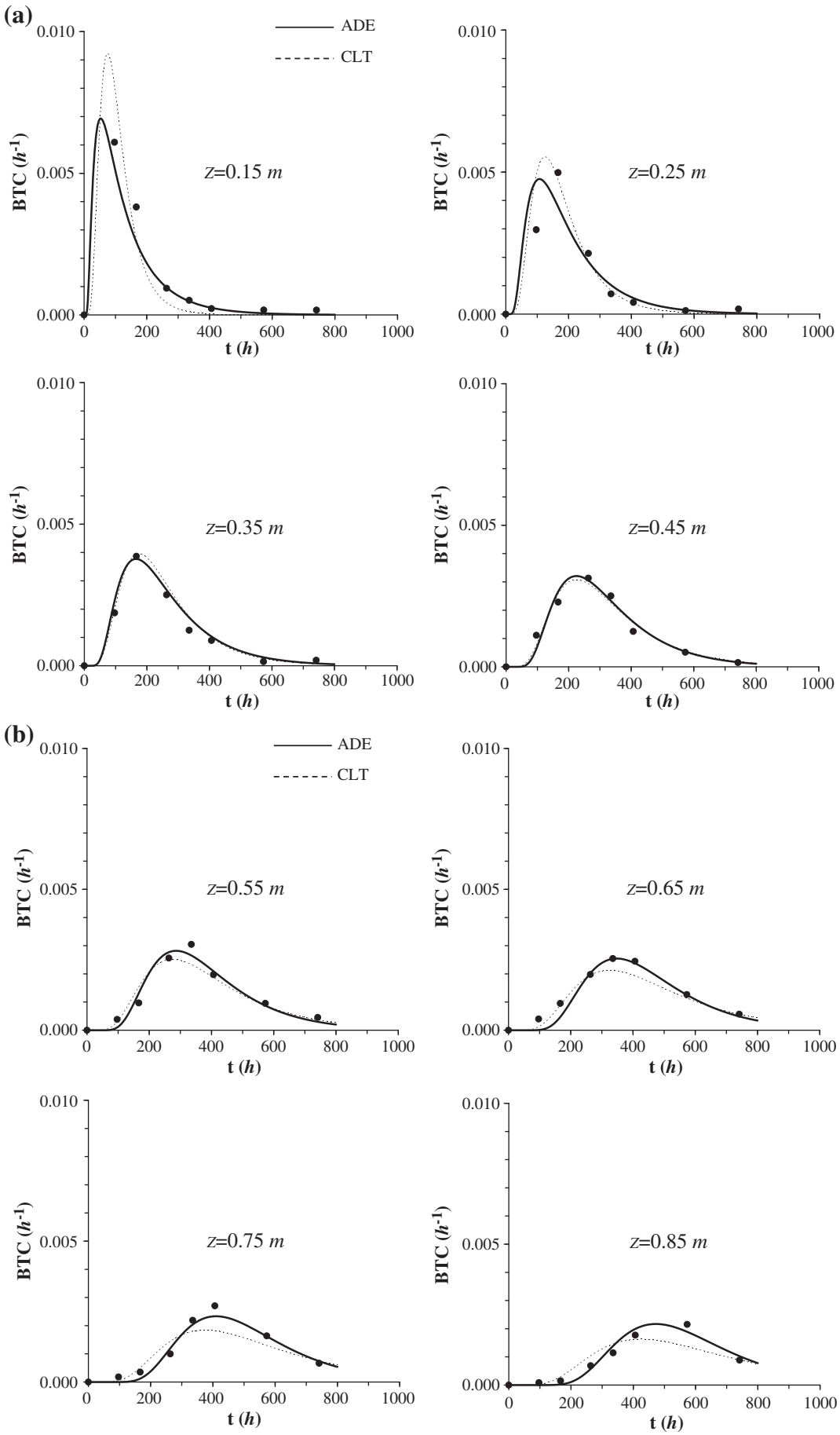
(a)
ADE
CLT
z=0.15 m
z=0.25 m
z=0.35 m
z=0.45 m
(b)
z=0.55 m
z=0.65 m
z=0.75 m
z=0.85 m
BTC (h-1)
t (h)
0.010
0.005
0.000
0
200
400
600
800
1000

Table 5
Maximum error (ME), root mean square error (RMSE) and model efficiency (EF) referring to measured and predicted mean concentrations.

Time (h)	*ME*		*RMSE* (%)		*EF*	
	CDE	CLT	CDE	CLT	CDE	CLT
97	2.81E−05	2.01E−03	36.3	57.5	0.93	0.90
167	1.72E−03	1.92E−03	53.0	48.4	0.79	0.87
263	4.54E−04	4.84E−04	18.5	17.2	0.96	0.97
335	1.39E−05	1.34E−04	0.5	5.5	1.00	1.00
407	3.61E−04	5.88E−04	18.4	25.8	0.95	0.87
573	4.45E−05	4.07E−06	17.4	20.4	0.94	0.91
742	1.97E−04	4.50E−04	17.5	36.9	0.96	0.78

treating the mean concentration distribution $\langle C(z,t)\rangle$ as (up to a constant) a probability density function, the solute spreading mechanism can be quantified by means of moments

$$Z_n^* = \frac{\int_0^\infty dz\, z^n \langle C(z,t)\rangle}{\int_0^\infty dz \langle C(z,t)\rangle} \qquad (n = 1, 2, \ldots). \tag{23}$$

While the ADE and CLT models account for a linearly increase with the depth z of the first-order moment $R_z = Z_1^*$, they provide a different characterization of the spreading mechanism [26]. Indeed, in the case of the ADE model, we shall look at the growth of the apparent dispersivity λ

$$\lambda = \frac{z}{2}\frac{\mathrm{Var}_z}{R_z^2} = \frac{z}{2}\mathrm{CV}_z^2 \tag{24}$$

(being $\mathrm{Var}_z = Z_2^* - R_z^2$ the variance). Alternatively, the apparent dispersivity (Eq. (24)) can be calculated from the optimized parameters at each depth, i.e. $\lambda = \frac{D}{U}$. Instead, in the case of the CLT model the spreading mechanism will be analyzed by looking at the standard deviation $\sigma_z = \sqrt{\mathrm{Var}_z}$. It is worth recalling here that, while λ grows with distance before reaching a constant (asymptotic) Fickian value for an advection-dispersion process [46], σ_z remains constant in the case of a process which obeys the CLT model [50].

In Fig. 6 the parameters λ and σ_z are depicted along the depth z. The dispersivity values (Fig. 6a), which are in agreement with values reported in the literature (see, e.g. [4]), are fairly constant with depth except for the shallowest ones. This suggests that, starting from $z \approx 0.50$ m, the concentration evolution can be regarded as a convection-dispersion process. In a different way, one could say that for the experiment under study the onset depth $\mathcal{Z}$ is around 45 cm. The transitional behavior from the soil surface $z = 0$ to $z = \mathcal{Z}$ is manifested into a growing dispersivity. It is instructive to show how our data-set can be coupled with theoretical results to come up with the formation heterogeneity statistical structure, which is a very difficult, and time consuming task (see, e.g. [37]). Indeed, it has been shown by Severino et al. [46] that for a soil that can be regarded as a bundle of non-interacting stream-tubes, the asymptotic macrodispersivity λ is

$$\lambda = \frac{D}{U} = I_v \sigma_Y^2 \exp(2\alpha\langle\Psi\rangle), \tag{25}$$

where I_v and σ_Y^2 represent the vertical integral scale and the variance of $Y = \ln K_s$, respectively, whereas $\langle\Psi\rangle$ is the mean head. The α-parameter depends upon the pore-size distribution, and it relates the hydraulic conductivity to the head [19]. One of the main advantages related to Eq. (25) is that it leads to a simple strategy to identify the heterogeneity structure. In fact, once $\langle\Psi\rangle$ and α are measured/estimated, one can easily infer $I_v\sigma_Y^2$. By considering that for the experiment at stake it turned out that $\lambda = \frac{D}{U} \simeq 6$ cm, $\langle\Psi\rangle \approx -210$ cm, $\sigma_Y^2 = \ln[1 + \mathrm{CV}^2(K_s)] \approx 0.84$, $\alpha \approx 0.001$ cm^{-1}, one gets $I_v \approx 10.8$ cm. Accounting for the fact (see Fig. 6a) that the Fickian regime is fully developed starting from $z \approx 50$ cm, we conclude that the macrodispersion mechanism becomes Fickian after that the center of gravity has travelled $\frac{50\ \mathrm{cm}}{10.8\ \mathrm{cm}} \approx 5$ vertical integral scales. This result is in excellent agreement with the theoretical predictions of Severino et al. [46]. It is important to emphasize that, although the analysis of Severino et al. [46] is based on linearization of the flow equations (and therefore it is formally restricted to formations with $\sigma_Y^2 \ll 1$), it is valid within a larger range of σ_Y^2 (for a detailed discussion, see [48]). As for the CLT model, it is seen that the variance σ_z^2 is practically constant along the depth (Fig. 6b). This is exactly the result one would expect from the transfer function theory (see, e.g. [50]), when the density probability distribution of the travel times follows the stochastic-convective model (Eq. (15)).

Before concluding, we wish to state here that the present paper has essentially focused on the use of mean concentration data. Nevertheless, the local values of the concentration are quite dispersed around the mean (Fig. 4). Rather than its practical implications, there is a definite theoretical interest (see, e.g. [18]) into quantifying fluctuations of local concentration values. To illustrate this point, in Table 5 we have reported the coefficient of variations of the chloride concentration. It is seen that the coefficient of variation may also be equal to 180%. Unlike the mean, the variance is strongly influenced by the mixing effects, which cause dilution [14]. This task, that to our knowledge has received less attention in the case of unsaturated media, is part of an ongoing project.

5. Concluding remarks

The experimental methodology described in this paper was successful in the acquisition of a comprehensive data-set describing nonreactive unsaturated solute transport at field-scale. The results indicate that at small depths (say for $z \le 0.40$ m) transport is still in the pre-asymptotic regime.

The very large fluctuations of local scale measurements represent one of the most striking features displayed by the concentration data. Nevertheless, the peak of the mean concentration appears to have been captured in all (except the final) sampling time. The mass recovery of the area-averaged pulse was near 100% at almost all the depths, with exception of two locations where it resulted slightly (i.e. 101.0%) in excess. This is presumably due to a residual chloride which was not completely removed during the flushing prior the salt application.

Two stochastic models were used to predict solute behavior. A scale effect was observed in the variance of the solute breakthrough curves, and in the relative medium dispersivity λ. The development of λ was more nearly proportional to the travelled distance (implying a linear growth of the dispersivity) with z. From the modelling point of view, this has a two-fold consequence. First, even if the ADE model could be in principle used to capture this growing macrodispersion effect, *de facto* it is not of practical use due to the impact of the boundary condition which cannot be neglected (it is reminded that the ADE model relies on the assumption of infinite medium). Second, the CLT (whose applicability is not limited to the assumption of infinite medium) is still poorly working since it assumes that transport takes place in a bundle of isolated vertical column, whereas the analysis of concentration data suggests that in the upper most depths lateral transport is not negligible. This implies that neither of the models could be calibrated at shallow depths, and predict transport accurately. For $z = 45$ cm, both the models provided an excellent representation of the spreading of the solute pulse, in agreement with the current stochastic theories.

Before concluding, we wish to emphasize that further investigations (along the lines of [18]) on the role of pore-scale dispersion are

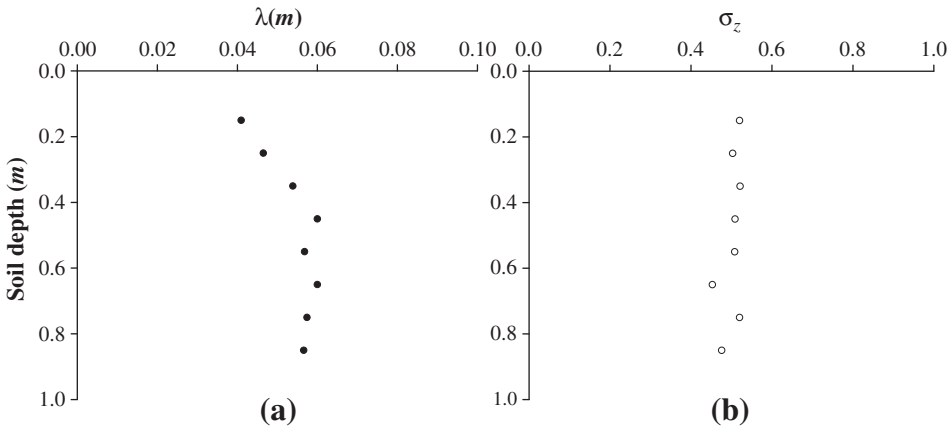

Fig. 6. Dispersivity λ (case a), and standard deviation σ_z (case b) versus the depth z.

needed to quantify the impact of local mixing mechanisms upon the concentration dilution in unsaturated porous media.

Acknowledgments

This study was supported by the grant: Methods for monitoring, predicting and controlling soil and groundwater pollution processes due to non-point agricultural sources (# MIUR 2007WA23ZC).

The suggestions from Gerardo Toraldo (University of Naples, ITALY) are kindly acknowledged. The constructive comments of two anonymous reviewers have significantly improved the early version of the paper.

References

[1] Amoozegar A, Warrick AW. Hydraulic conductivity of saturated soils: field methods. In: Klute A, editor. Methods of soil analysis. Part 1. Physical and mineralogical methods; 1986.
[2] Bear J. Dynamics of fluids in porous media. Dover; 1972.
[3] Beven K, Germann P. Macropores and water flow in soils. Water Resour Res 1982;18:1311–25.
[4] Beven K, Henolerson DE, Reeves AD. Dispersion parameters for undisturbed partially saturated soil. J Hydrol 1993;143:19–44.
[5] Butters LG, Jury WA, Frederick FE. Field scale transport of bromide in an unsaturated soil 1. Experimental methodology and results. Water Resour Res 1989;25:1575–81.
[6] Butters LG, Jury WA. Field scale transport of bromide in an unsaturated soil: 2 Dispersion modeling. Water Resour Res 1989;25:1583–9.
[7] Comegna V, Coppola A, Sommella A. Effectiveness of equilibrium and physical non-equilibrium approaches for interpreting solute transport through undisturbed soil columns. J Contam Hydrol 2001;50:121–38.
[8] Costa JL, Knighton RE, Prunty L. Model comparison of unsaturated steady-state solute transport in a field plot. Soil Sci Soc Am J 1994;58:1277–87.
[9] Cui J, Zhuang J. Solute transport in cinnamon soil: measurement and simulation using stochastic models. Agric Water Manage 2000;46:43–53.
[10] Dagan G. Solute transport in heterogeneous porous fonnations. J Fluid Mech 1984;145:151–77.
[11] Dagan G. Statistical theory of groundwater flow and transport: pore to laboratory, laboratory to formation, and formation to regional scale. Water Resour Res 1986;22:120S–34S.
[12] Dagan G. Flow and transport in porous formations. Springer-Verlag; 1989.
[13] Dagan G, Neuman SP. Subsurface flow and transport: a stochastic approach. Cambridge University Press; 1997.
[14] Dagan G, Fiori A. The influence of pore-scale dispersion on concentration statistical moments in transport through heterogeneous aquifers. Water Resour Res 1997;33:1595–605.
[15] Dagan G. On application of stochastic modeling of groundwater flow and transport. Stoch Environ Res Risk Assess 2004;18:266–7, doi:10.1007/s00477-004-0191-7.
[16] Dentz M, Tartakovsky DM. Self-consistent four-point closure for transport in steady random flows. Phys Rev E 2008;77:066307.
[17] Ellsworth TR, Jury WA, Ernst FF, Shouse PJ. A three-dimensional field study of solute transport through unsaturated, layered, porous media methodology, mass recovery, and mean transport. Water Resour Res 1991;27:951–65.
[18] Fiori A, Dagan G. Concentration fluctuations in aquifer transport: a rigorous first-order solution and applications. J Contam Hydrol 2000;45:139–63.
[19] Gardner WR. Some steady state solutions of unsaturated moisture flow equations with application to evaporation from a water table. Soil Sci 1958;85:228–32.
[20] Gasser MO, Caron MR. Solute transport modelling under cultivated sandy soils and transient regime. J Environ Qual 2002;31:1722–30.
[21] Gee GW, Or D. Particle size analysis. In: Done JH, Topp GC, editors. Methods of soil analysis. Part 4. Phys. methods. Madison, WI: SSSA; 2002. p. 255–93.
[22] Gelhar LW. Stochastic subsurface hydrology. Prentice Hall; 1993.
[23] Heuvelman WJ, McInnes K. Solute travel time distributions in soil: a field study. Soil Sci 1999;164:2–9.
[24] Jacques D, Kim D, Diels J, Vanderborght J, Vereecken H, Feyen J. Analysis of steady state chloride transport through two heterogeneous field soils. Water Resour Res 1998;34:2539–50.
[25] Jury WA. Simulation of transport using a transfer function model. Water Resour Res 1982;18:363–8.
[26] Jury A, Roth K. Transfer functions and solute movement through soil. Birckhäuser-Verlag; 1990.
[27] Kachanosky RG, Pringle E, Ward A. Field measurement of solute travel time using time domain reflectometry. Soil Sci Soc Am J 1992;56:47–52.
[28] Kim DJ, Feyen J. Comparison of flux and resident concentrations in macroporous soils. Soil Sci 2000;8:616–23.
[29] Loague K, Green R.E. Criteria for evaluating pesticide leaching models. Field-scale and solute flux in soils. P 175-207. In Proc Centro Stefano Fraschini Ascona, Monte Verità, 24-29 Sept. Birkhauser Verlag, Basel, Switzerland.
[30] Nelson DW, Sommers LE. Total carbon organic carbon and organic matter. In: Page AC, et al, editor. Methods of soil analysis, Part 2. Chemical and microbiologically properties. ASA; 1982. p. 539–79.
[31] Neuman SP. Stochastic groundwater models in practice. Stoch Environ Res Risk Assess 2004;18:268–70, doi:10.1007/s00477-004-0192-6.
[32] Neuman SP, Tartakovsky DM. Perspective on theories of non-Fickian transport in heterogeneous media. Adv Water Resour 2009;32:670–80, doi:10.1016/j.advwatres.2008.08.005.
[33] Radcliffe DE, Gupta SM, Box JE. Solute transport at the pedon and polipedon scales. Nutr Cycl Agroecosyst 1998;50:77–84.
[34] Ragab R, Cooper JD. Variability of unsaturated zone water transport parameters: implications for hydrological modelling, 1. In-situ measurements. J Hydrol 1993;148:109–31.
[35] Reynolds WD, Elrick DE. In-situ measurement of field-saturated hydraulic conductivity, sorptivity, and the a-parameter using the Guelph permeameter. Soil Sci 1985;140:292–302.
[36] Roth K, Jury W, Fluhler H, Attinger W. Transport of chloride trough an unsaturated field soil. Water Resour Res 1991;27:2533–41.
[37] Rubin Y. Applied stochastic hydrology. Oxford University Press; 2003.
[38] Russo D, Bouton M. Statistical analysis of spatial variability in unsaturated flow parameters. Water Resour Res 1992;28:1911–25.
[39] Russo D. Stochastic modeling of macrodispersion for solute transport in a heterogeneous unsaturated porous formation. Water Resour Res 1993;29:383–97.
[40] Russo D. On the velocity covariance and transport modeling in heterogeneous anisotropic porous formations 2. Unsaturated flow. Water Resour Res 1995;31:139–45.
[41] Russo D, Russo I, Laufer A. On the spatial variability of parameters of the unsaturated hydraulic conductivity. Water Resour Res 1997;33:947–56.
[42] Russo D. Stochastic analysis of flow and transport in unsaturated heterogeneous porous formations: effects of variability in water saturation. Water Resour Res 1998;34:569–81.
[43] Sardin M, Schweich D, Leij FJ, van Genuchten MTh. Modelling the nonequilibrium transport of linearly interacting solutes in porous media: a review. Water Resour Res 1991;27:2287–307.
[44] Schulin R, Wierenga PJ, Fluher H, Leuenberger J. Solute transport through a stony soil. Soil Sci Soc Am J 1987;51:36–42.

[45] Severino G, Santini A, Sommella A. Determining the soil hydraulic conductivity by means of a field scale internal drainage. J Hydrol 2003;273:234–48.
[46] Severino G, Santini A, Monetti VM. Modelling water flow and solute transport in heterogeneous unsaturated porous media. In: Pardalos, Papajorgji, editors. Advances in modelling agricultural systems. Springer; 2009. p. 361–83, doi: 10.1007/978-0-387-75181-8_17.
[47] Taylor GI. Diffusion by continuous movements. Proc Lond Math Soc 1921;20: 196–212.
[48] Tartakovsky DM, Guadagnini A, Riva M. Stochastic averaging of nonlinear flows in heterogeneous porous media. J Fluid Mech 2003;492:47–62.
[49] Ünlü K, Nielsen DR, Biggar JW, Morkoc F. Statistical parameters characterizing the spatial variability of selected soil hydraulic properties. Soil Sci Soc Am J 1990;54: 1537–47.
[50] Vanderborght J, Gonzalez C, Vanclooster M, Mallants M, Feyen J. Effects of soil type and water flux on solute transport. Soil Sci Soc Am J 1997;61:372–89.
[51] White I, Sully MJ. On the variability and use of the hydraulic conductivity alpha parameter in stochastic treatment of unsaturated flow. Water Resour Res 1992;28:209–13.
[52] Zhang R, Yang J, Ye Z. Solute transport through the vadose zone: a field study and stochastic analyses. Soil Sci 1996;16:270–7.